The Journal of the Oceanological Society of Korea
Vol. 16, No. 1, 12-23, June 1981

NUMERICAL MODELLING OF THE COASTAL UPWELLING NEAR THE POLEWARD EDGE OF THE WESTERN BOUNDARY CURRENT

Hui Soo An
Dept. of Earth Science, Seoul National University

ABSTRACT

A numerical experiment is made in order to clarify the mechanism of the upwelling phenomenon along the coast near the poleward edge of the western boundary current. The possibility of the upwelling is suggested from the analysis of the observational data in the east of Honshu, Japan, and in the south eastern coast of Korean Peninsula. This upwelling phenomenon is very deep and can be traced to the bottom layer. The upwelling phenomenon seems to be a general oceanic feature which characterizes the region along the west coast near the poleward edge of the western boundary current. This experiment is simulating the oceanic condition of the transition region between Kuroshio front and the Oyashio front in the east of Honshu, Japan.

The possible explanations of the causes of the upwelling are as follows; In the interior of the modeled ocean the cold heavy water supplied from the north and the warm light water from the south make the north-south gradient of the pressure field and accelerate the eastward current to produce the h-orizontal divergence field near the west coast. The divergence is compensated by the upwelling near the separation region. Another one is that the upwell-ed cold water strengthen constantly the pressure gradient which is balanced by the northward current and is weakened by the horizontal diffusion.

INTRODUCTION

We showed the evidence of the existence of the upwelling in the region between the Kuroshio and the coast from Ibaragi to Fukushima prefecture by using data of serial observations in the east of Honshu (An, 1980 a).

Recently, many attempts of numerical experiments of the Kuroshio or the western boundary current have been made for the purpose of understanding the mechanism of the large scale meandering of the Kuroshio or the appearance of the large cold water off the Enshunada. Some of the results of such work indicate the sign of the existence of the upwelling phenomenon in the region along the coast near the poleward edge of the western boundary current e.g. Takeuchi ((Fig. 9), 1977) and Robinson *et al.* ((Fig. 11), 1976).

The purpose of this paper is to clarify the mechanism of such upwelling phenomenon through a numerical experiment by using a simple model which seems to represent the basic oceanic conditions near the poleward edge of the western boundary current. Especially this model simulates the oceanic condition of the transition region between the Kuroshio front and the Oyashio front.

USED MODEL

The schematic view of the modeled ocean in this study is shown in Fig. 1. For simplicity,

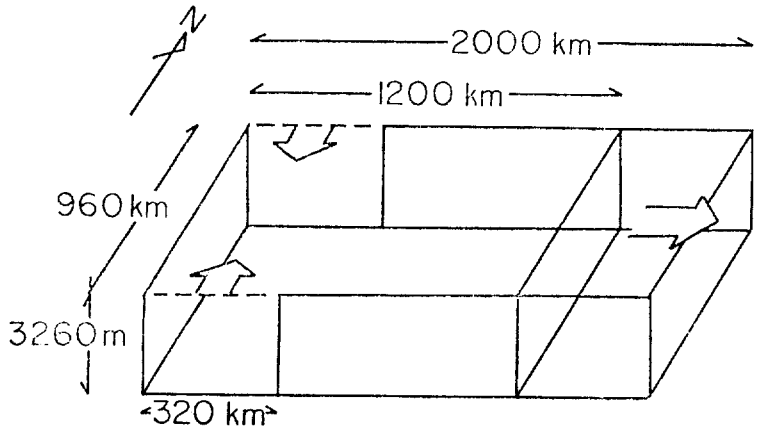

Fig 1. Schematic view of the modeled ocean.

we consider a rectangular ocean of uniform depth. The western wall of the ocean is assumed to correspond to the western boundary of the real ocean such as the coast of Japan in the case of the Pacific Ocean, and we apply non-slip condition on this western wall. We select the north-south scale of the ocean to be 960 km in order that the interfrontal zone between the Kuroshio and Oyashio fronts having the scale of about 500 km can be represented inside it. The slippery boundary conditions are adopted on the southern and northern walls. The openings of 320 km width are set on the western edges of the southern and northern walls in order to give the southern and northern inflows, respectively. The eastern boundary of the ocean is opened. The distributions of temperature, salinity and velocity are assumed to be constant on this open boundary. Total outflow through the eastern boundary is set to be just equal to the sum of inflows through the northern and southern openings. The vertical profile of the eastward velocity is not fixed but the eastward transport (integrated value of eastward velocity along z-axis) is fixed to be constant along the eastern open boundary in the first stage of the calculation. The east-west scale of the ocean is set to be 2000 km in the first stage of the calculation with coarse mesh (80 km), and to be 1200 km in the second stage with fine mesh (40 km). The depth of the modeled ocean is taken to be 3260 m for the convenience of calculations, and the slippery boundary condition is applied on this artificial bottom. The rigid lid approximation is used on the sea surface. No thermal and momentum fluxes are allowed through the surface, bottom and vertical walls except the above mentioned three openings.

The distributions of temperature, salinity, sigma-t and velocity which are imposed on the southern and northern openings are based on the cross sections of the Kuroshio extension measured by Kofu-maru, Japan Meteorological Agency, along the longitude of 144°E in the winter 1967, and those of the Oyashio measured also by Kofu-maru along the latitude of 41.5°N in the winter 1965, respectively. The velocity is assumed to be normal to the opening surfaces, and its distributions are determined so as to satisfy geostrophic relation (thermal wind relation). We put the constant velocities along the bottom and adjusted the total transport through the southern opening (Kuroshio) and the northern opening (Oyashio) to be 50×10^6 m^3/sec, and 10×10^6 m^3/sec respectively. So the total transport through the eastern open boundary is 60×10^6 m^3/sec.

We start the calculation from the uniformly stratified ocean which are based on the observational data obtained in the subarctic water region off the southeastern coast of Hokkaido. In order to minimize the disturbances resulted from the discrepancy between the initial profile and the profiles to be imposed on the southern and northern openings, the boundary values on the openings are given by

$$[T(x,z)-T_0(z)]\tanh(t/\tau)+T_0(z)$$

and

$$[S(x,z)-S_0(z)]\tanh(t/\tau)+S_0(z),$$

where $T(x,z)$ and $S(x,z)$ are the distributions to be imposed on the southern and northern openings, and $T_0(z)$ and $S_0(z)$ the profiles of the temperature and salinity given initially in the interior of the modeled ocean, respectively. The time constant τ is selected to be 6 months, and so the boundary conditions at these opening can be considered as fixed after 6 months from the begining of the calculation.

We select the horizontal grid of 80 km and time step of 4 hours in the first stage of the calculation. Almost steady flow pattern is achieved after about 17 years (6118 days), and then we go into the second stage of the calculation using finer horizontal grid size (40 km) and finer time step (2 hours).

We used 8 layered model both in the first and second stages of the calculation. Thicknesses of the layers are selected to be 40 m, 50 m, 70 m, 100 m, 200 m, 400 mg, 800 m, and 1600m from top to bottom. In the second stage, the eastern boundary is taken at the distance of 1200 km from the west coast. The initial conditions for the calculation of the second stage are given from the interpolations of the results of the first stage calculation. Then the functional form of the eastward transport on the eastern open boundary is fixed throughout the calculation of the second stage. The calculation of the second stage is conducted for about 5 years (1837 days) untill almost steady flow pattern is achieved. The detailed discription about the calculation is explained by An (1980. b)

RESULTS

1. General feature of the oceanic conditions represented in the modeled ocean.

The horizontal distributions of temperature, salinity and sigma-t for the first layer (0-40 m) and the seventh layer (860-1660 m) on the firststage are shown in Fig. 2, and the stream function and velocity field for the first and seventh layers are shown in Fig. 3. The corresponding results on the second stage are shown in Figs. 4 and 5. Roughly speaking, the obtained results have the characteristics of the ocean of two layered type, and so the first and seventh layers are selected as representatives of surface layers and bottom layers, respectively. In the results on the first stage, the water of low temperature and low salinity extends eastwards from the northern opening. The center (local minimum of temperature and salinity in north-south direction) of this water tongue of low temperature and low salinity is shown by dashed line in each figures. Here, we shall confine our attention only to the region south of the center of the cold and less saline water tongue. Except the northern half of this water tongue, the temperature and salinity are generally decreasing towards north in the first layer.

There exists sharp temperature and salinity fronts near the north-west corner of the modeled ocean. Such a sharp front may correspond to the Oyashio front in the real ocean. According to the sharp temperature and salinity fronts, strong northeastward current is generated in the first layer just south of the east edge of the northern opening. The current is partly connected with southern northward current related to the meandering of the Kuroshio extension,

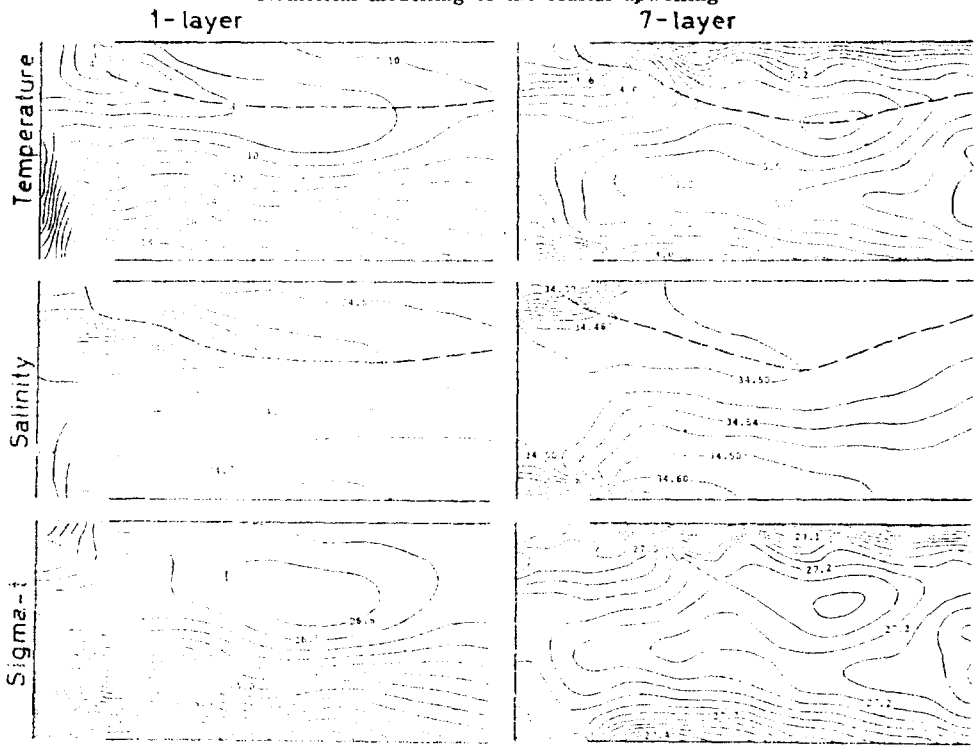

Fig. 2. The horizontal distributions of temperature, salinity and sigma-t for the first layer (0-40 m) and the seventh layer (860-1660 m) on the first stage.

and seems to cause the abnormally large meandering of the Kuroshio extention in the surface layers in the results on the second stage. Why the Oyashio front is confined near the northwest corner of the modeled ocean is not clear. However, as seen in the figure of the stream function (Fig. 5), the front is related to the existence of the strong clockwise gyre located along the central part of the northern boundary. The strength of the gyre does not show the periodical change with period about 220 days which can be seen in the curve of energy evolution (Fig. 6), while the other southern gyres or vortexes change their strength periodically. So, it seems to be reasonable to think that this clockwise gyre does not receive their vorticity from the meandering of the southern Kuroshio current. This clockwise gyre is strongly related with the current systems of the bottom layers as seen from the comparison with current fields of the seventh layer. The bottom

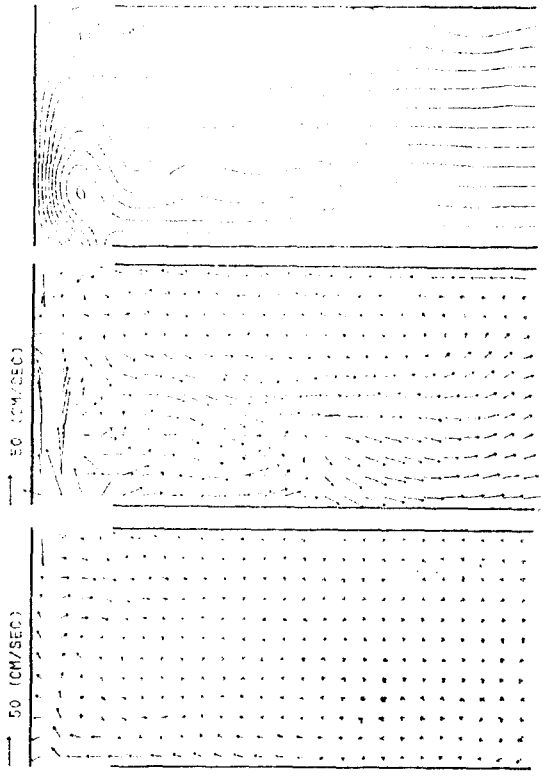

Fig. 3. The stream function and the velocity field for the first and seventh layers on the first stage.

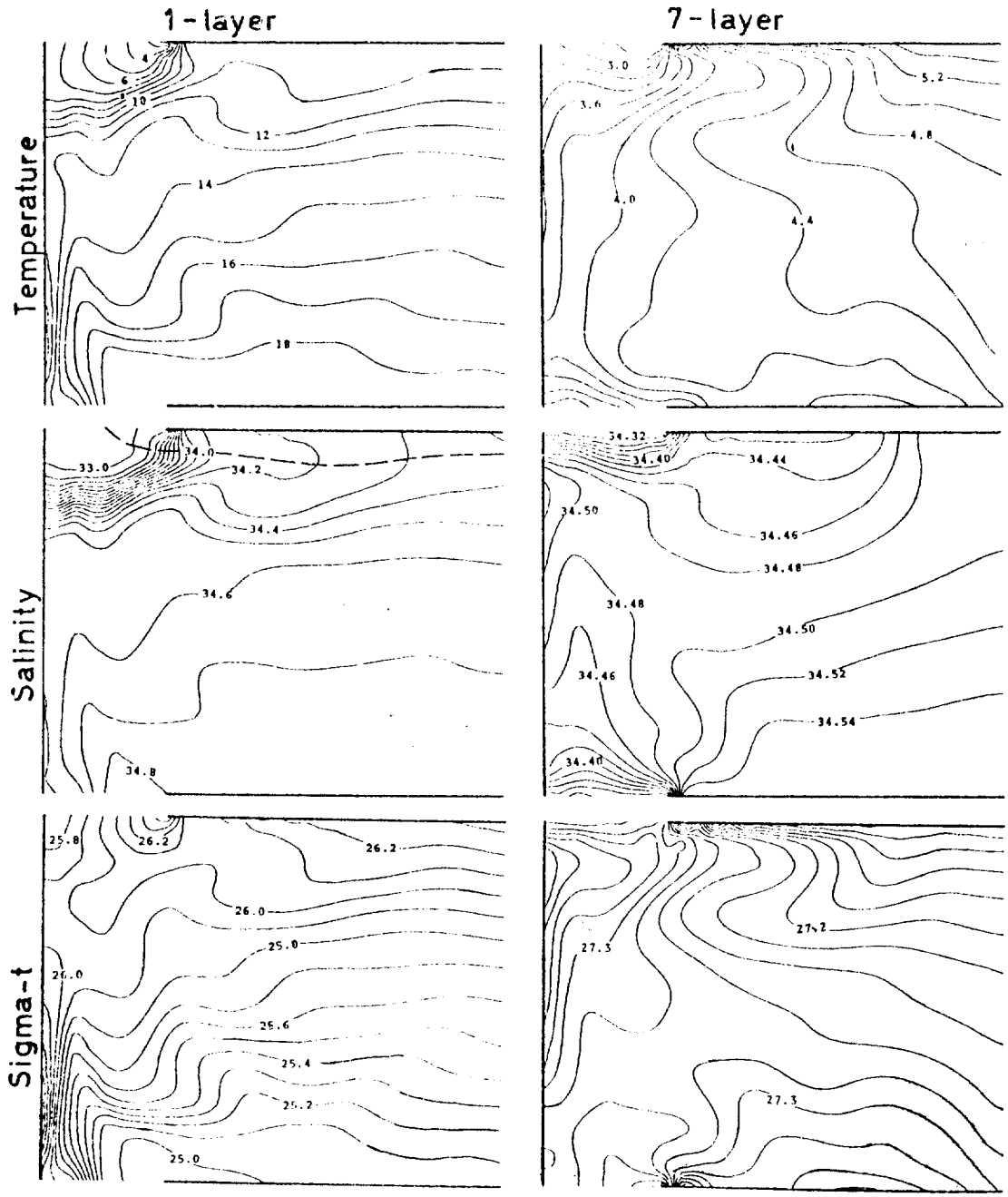

Fig. 4. The horizontal distributions of temperature, salinity and sigma-t for the first layer (0-40m) and the seventh layer (860-1660 m)

current at the eastern open boundary is westward at northern several points. This inflow through the eastern open boundary seems to strengthen the clockwise gyre in the bottom layers. In the second stage of calculation, we need to set the eastern open boundary at 1200 km from the west coast due to the restriction on the computation. The results on the second stage seems to be

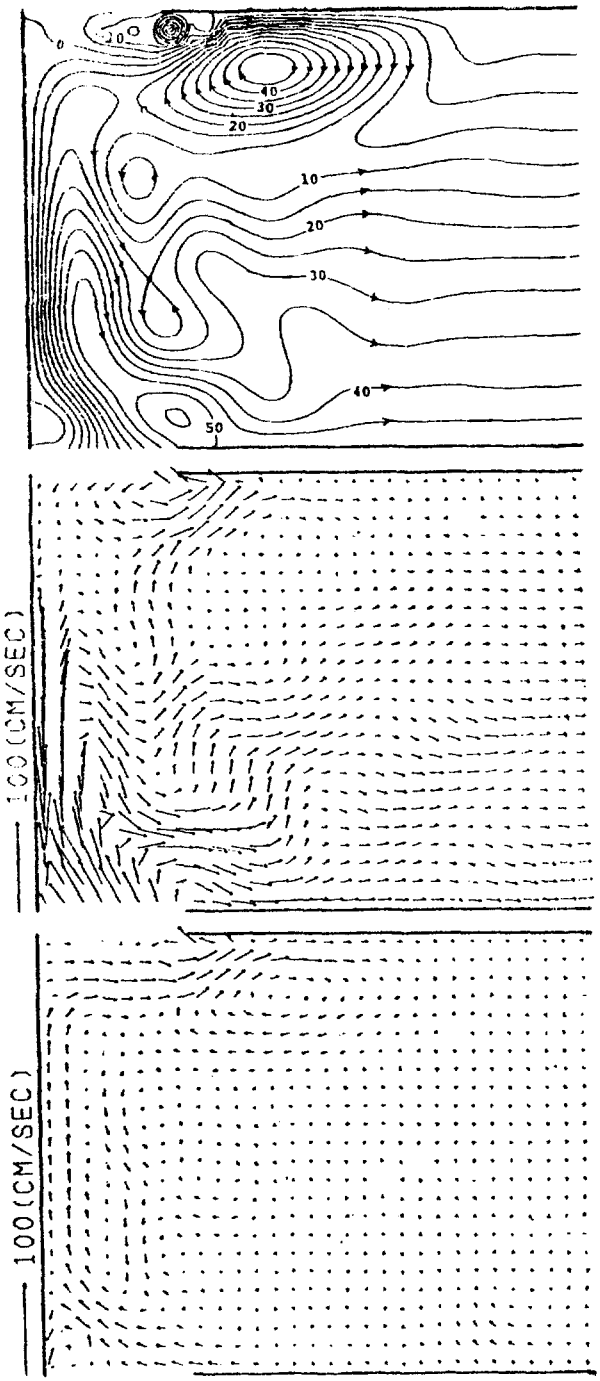

Fig. 5. The stream function and the velocity field for the first and seventh layers on the second stage.

affected not only by the inadequate boundary conditions on the northern wall but also by those on the eastern open boundary.

However, if we confine our attention to the behavior of the western boundary current or the Kuroshio, the modelling of the oceanic conditions is not so wrong as seen in the results on the first stage and on the second stage. The current, the axis of which is given a little offshorewards on the southern opening, shifts to west and soon shows the characteristics of the western boundary current. Then it gradually leaves the west coast and flows eastwards after exhibiting the large meanderings.

2. Coastal upwelling near the poleward edge of the western boundary current.

One of the distinguished features which can be seen both in the results on the first stage and on the second stage is the existence of the low temperature, low salinity and high-density region along the coast near the edge of the western boundary currents in the surface layers.

The position of this isolated high density region on the first stage is a little northward than that on the second stage. The location of the center of the high density region is very near of north of the point where the current axis of the Kuroshio approaches nearest to the coast. The velocity field in northsouth cross section at the distance of 40 km from the west coast on the first stage and that at the distance of 20 km from the second stage are shown in Fig. 7. As seen from these figures, the region of the isolated high density just corresponds to that of upwellings. It should be noted that the upwelling phenomenon can be recognized even in the eighth (bottom) layer. The velocity fields in east-west cross section at the distance of 200 km from the southern boundary on the first stage and that at the distance of 220 km from the southern boundary on the second stage are shown in Fig. 8. As seen from these figures, the upwelling phenomenon is confined very near the west coast. The basic characteristic of this

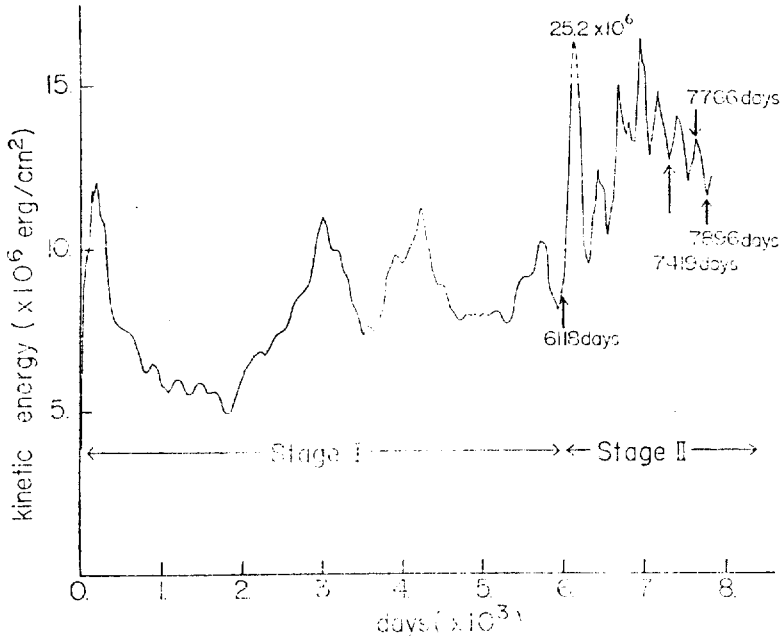

Fig 6. Evolution of the kinetic energy in the modeled ocean. The averaged kinetic energy per unit area (erg/cm^2) is taken in ordinate and the time (days) is taken in abscissa. In the calculation, we used coarse mesh (80 km) for the first 6118 days (Stage I) and fine mesh (40 km) for the later 1837 days (Stage II). The numbers in the figure indicate the days when we show the results of the calculation.

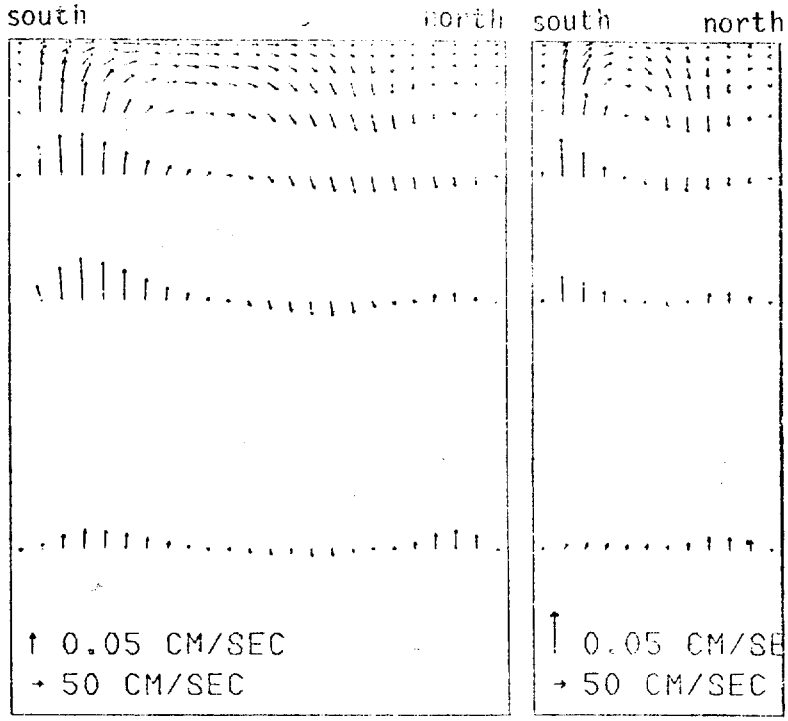

Fig 7. The velocity field in north-south cross section at the distance of 40 km from the west coast on the first stage (right) and that at the distance of 20 km from the west coast on the second stage (left).

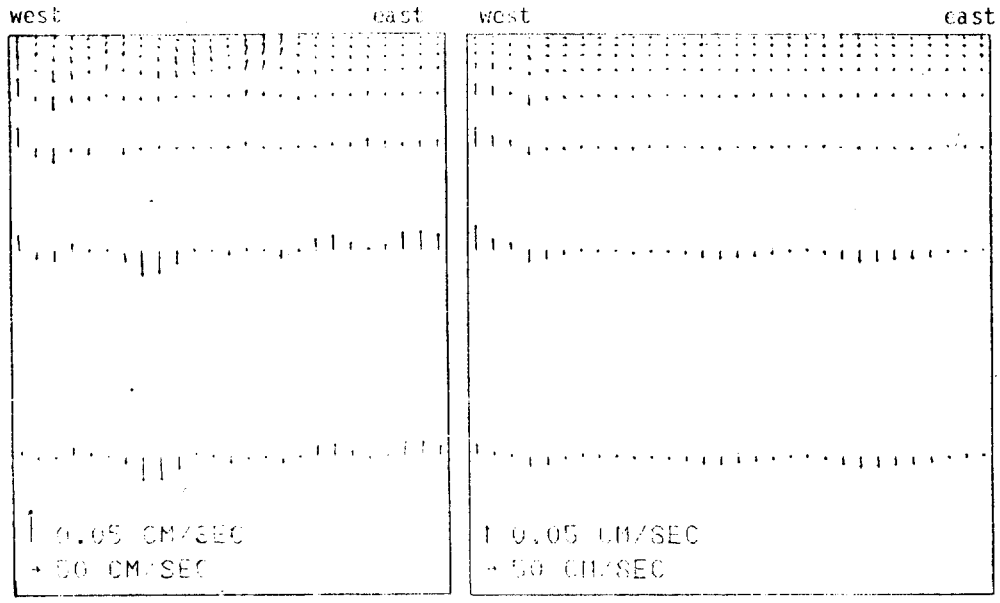

Fig 8. The velocity fields in east-west cross section at the distance of 200 km from the southern boundary on the first stage (left) and that at the distance of 220 km from the southern boundary on the second stage (right).

upwelling phenomenon is, therefore, very similar to that of the upwelling phenomenon observed just off the coast from Ibaragi to Fukushima prefecture which was discussed by An (1980, a).

In the north-south cross sections, we can see the downwelling region further north of the upwelling region. The position of the downwel ling region corresponds to that of the sharp temperature and salinity front (the Oyashio front). It seems to reasonably understood that the low temperature and low salinity water supplied through northern opening may descend along the Oyashio front. The existence of such a downwelling region in the real ocean is not clear. So, if the downwelling is resulted from the inadequacy of the used simple model, the southern upwelling region discussed above may be exaggerated in our model, because the torque which is given by the supply of the Oyashio water through northern opening may produce a convective motion in the north-south cross section.

In the east-west cross section, we can see that the upwelling is limited within the narrow region near the west coast, and that the downwelling region is existed just offshore of the upwelling region. This east-west gradient of the vertical velocity seems to act to maintain the east-west gradients in temperature and salinity distribution and so in pressure field against to smoothing action due to the eddy diffusions. As the property of the current in the model is basically geostrophic, the upwelling along the coast might be a necessary condition to existence of the strong boundary currents.

Godfrey (1973 a and b) discussed the upwelling phenomenon near the poleward edge of the western boundary current in connection to the fluctuation of the flow patterns or the eddies.

The upwelling discussed in this paper seems to be of steady state phenomenon. Though the conclusions on the detailed process and mecha-

nism of the upwelling is very hard to be derived from the results of the limited numerical experiments, one of the possible explanation of the cause of the upwelling is as follow. In the interior of the modeled ocean, the Oyashio waters supplied from the northern opening is located northward and the Kuroshio waters from the southern opening located southward. The resultant north-south gradient of the pressure field has the tendency to accelerate the eastward current and may produce the horizontal divergence field near the west coast. Or, more simply, when the strong western boundary current shift its flow direction offshore, it may entrain the waters near the coast to produce the divergence field there. Then, the divergence field would generate the upwelling near the coast. In this case, the upwelling phenomenon should be traced to depths where the considerable current velocity of the western boundary current can be recognized.

DISCUSSION

We see the evolution of the vertical velocity in the upwelling region in Fig. 9. The maximum vertical velocity at grid points nearest to the west coast (at 40 km from the coast in the first stage of the calculation and at 20 km in the second stage of the calculation) at the depth of 360 m is shown in this figure. In the later part of the second stage calculation, the evolution curve of the upwelling velocity shows the variation with period of about 220 days just as that of the total kinetic energy in the modeled ocean (Fig. 6). The phase of the upwelling velocity has the tendency to preceed that of the kinetic energy. The amplitude of the periodic variation is decaying slowly and steadily, so that we expect the existence of the steady state solution. The average level of the upwelling velocity seems to be steady in the end of the second stage calculation, while

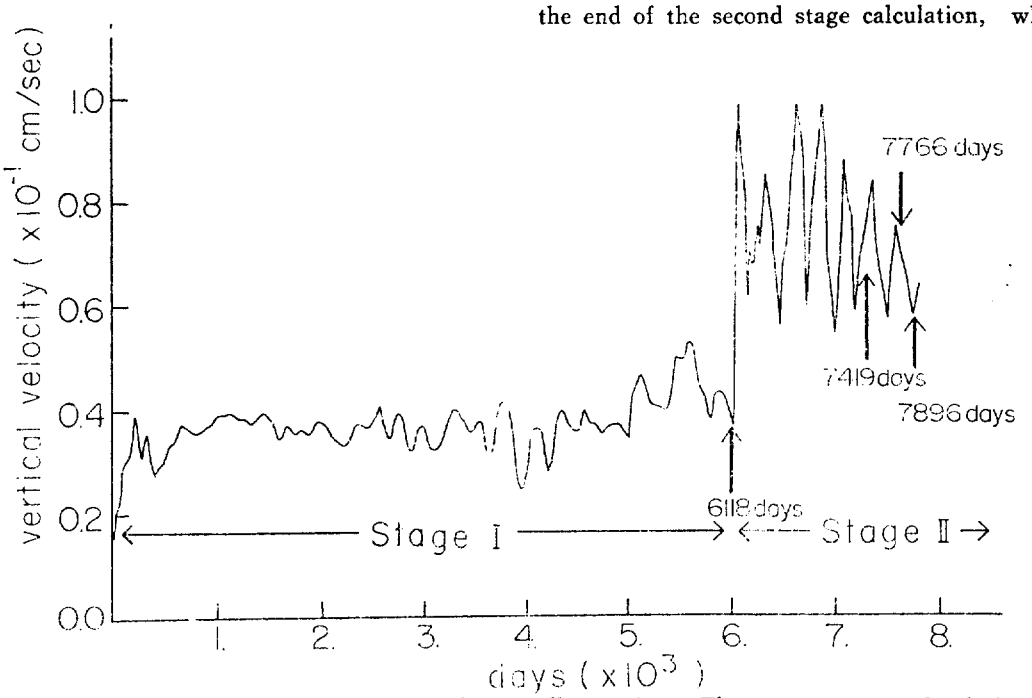

Fig. 9. Evolution of the vertical velocity in the upwelling regions. The maximum vertical velocity in grid points nearest to the west coast (at 40 km from the coast in the first stage of the calculation and at 20 km in the second stage of the calculation) at the depth of 360 m is shown.

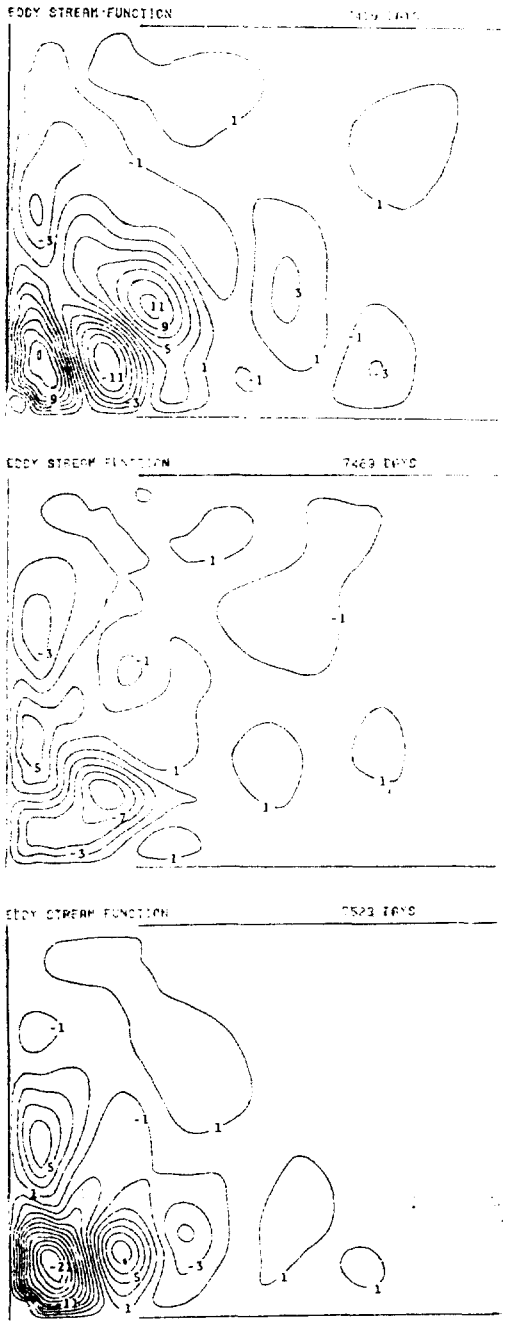

Fig. 10. The deviations of the transport stream function from the averaged values over the period from 7419th day. Upper figures show the deviations on 7419th day, middle on 7469th day and lower on 7523rd day.

that of the kinetic energy has yet the tendency to decrease.

In Fig. 10, the deviations of the transport stream function from the averaged values over the period from 7419th day to 7618th day are shown for 7419th day, 7469th day and 7523th day, respectively. We can see several eddies are generated in the southeast parts of the modeled ocean, and some of them move northeastward. The upwelling also varies. It should be noted that the periodic components of 220 days are very small in the northern portion which is precluded from the discussions in the above section. The center of the water of low temperature and low salinity from the northern opening shifts southwards toward east, and values of the center up to the northern walls. Therefore, the northern part of the ocean beyond the center of the cold and less-saline water tongue is not suitable as the model of the subarctic ocean. Due to these abnormal temperature and salinity distributions near the northern boundary, the strong westward current is generated along the northern boundary. This unsuitable feature seems to be resulted from the deficit of the supply of the Oyashio water from the northern opening, and so the cold and less-saline water regions along the northern walls cannot be established. In order to improve the situation near the northern boundary, it should be needed to use more reasonable boundary condition at the northern boundary. At least, we should use the model which allows the outflow of the heat and salinity through the northern wall due to the diffusion process.

The east-west scale of the front in the modeled ocean is comparable with the width of the northern opening. Therefore, the modeling of the subarctic ocean is not succeeded in the northern part of the modeled ocean except near the western boundary. The northern one-third of the modeled ocean including the region of the strong clockwise gyre should be excluded from our discussions except near the west coast.

Besides, the local vortexes seen just near the eastern edges of the southern and northern opening may be affected by the inadequacy of the boundary conditions imposed on the open boundaries.

Since the most determinative factor in our model is the inflow of the momentum, heat and salinity through the southern opening, it should be reasonable to confine our attention mainly to the southwestern parts of the modeled ocean or to the vicinity of the western boundary currents.

The strength of the strong clockwise gyre located along the central part of the northern boundary has the tendency to vary with longer time scale just corresponding to the change of the averaged level of the periodical variation of 220 days. Therefore, the change of the averaged level of the kinetic energy may be influenced by the erroneous boundary conditions. The periodic variation in the upwelling velocity might be considered as a good sign that the computational results is not so affected from the erroneous boundary conditions, though it gives some difficulties to estimate the steady stage conditions. Because of the steadiness of the averaged level of the upwelling velocity curve at the end of the second stage calculation, we feel that the results on the upwelling phenomenon along the coast near the poleward edge of the western boundary current is reliable enough, though we had to terminate the calculation on 7955th day.

CONCLUSION

We try to reproduce numerically the upwelling phenomenon along the coast near the poleward edge of the western boundary current in the modeled ocean. Though the oceanic conditions in the vicinity of the Oyashio front cannot be reproduced in our simple model with artificial boundary conditions on the northern and eastern boundaries, the existence of the upwelling is clearly shown along the coast near the poleward edge of the western boundary current. This upwelling phenomenon is very deep, and can be traced to the bottom layer. Though the more elaborated experiments would be needed to know the detailed mechanism, the upwelling phenomenon seems to be a general oceanic feature which characterize the region along the west coast near the poleward edge of the western boundary current in the ocean.

ACKNOWLEDGEMENT

The author wishes to express his heartful thanks to the late Professor Kozo Yoshida for his guidance and encouragement in this study. He also wishes to express his thanks to Professor Yutaka Nagata and Professor Nobuo Suginohara of Tokyo University for their advice, discussions and guidances.

REFERENCES

An, H.S. 1974. On the cold water mass around the south east coast of Korean Peninsula. J. Oceanolo. Soc. Korea, 9:10-18.

An, H.S. 1980a. Observational evidence of the upwelling off Cape Shioyazaki in Fukushima Prefecture, Japan. J. Oceanogr. Soc. Japan, 36:85-95.

An, H.S. 1980b. Finite difference method for the ocean with the density stratification. Bull. KORDI, 2:1-7.

Godfrey, J.S. 1973. On the dynamics of the western boundary current in Bryan and Cox's (1968) numerical model ocean. Deep Sea Research, 20:1043-1058.

Godfrey, J.S. 1973. Comparison of the East Australian Current with the western boundary flow in Bryan and Cox's (1968) numerical model ocean. Deep Sea Research, 20:1059-1076.

Robinson, A.R., D.E. Harrison, Y. Mintz and A.J.

Semtner 1976. Eddies and the general circulation of an idealized ocean gyre: A wind and thermally driven primitive equation numerical experiment. J. Phys. Oceanogr., 7:182-207.

Takeuchi, K. 1977. Numerical experiment on subtropical gyre. Marine Sci. Monthly, 9:54-60.